AFTERNOON SESSION

MR. ALFRED KAHAN, Rome Air Development Center

This afternoon session considers improved timing devices, namely Rubidium Frequency Standards, and a continuation of a topic of Synchronization.

Several years ago, I think it was in 1978, according to the proceedings of this conference, I made some remarks, during one of the panel sessions regarding the lack of research and development in rubidium frequency standards. And even the possible obsolescence of the standard.

Clark oscillators promise quantum improvements and cesium standards were suppose to become smaller and cheaper, and rubidium was being squeezed in the middle. At that time, and since then I have received severe reaction to those comments, and I think in this same spirit the organizing committee considered it poetic justice that I should chair this session on R&D and Rubidium Frequency Standards.

Before I call the first paper, I would like to relate to you an incident I had this weekend. I was over at some friend's house and she showed me a collector's bound volume of the illustrative London News from 1871, which was a beautiful copy of a combination of life and time type of thing of today. Today it has a little bit of times, a little bit of sports, and has everything else. In that one it was related that, in the June 3rd issue of 1871 that was called clocks and photographs. And evidently Mr. Norman Lockyer, who I'm told by Dr. Winkler is a known astronomer, gave his sixth lecture on instrumentation using modern astronomy, that was devoted to clocks and photographs, as such. And he went on to review the history of the development of clocks starting with Archimedes and the wheels moved by weight. And then he mentioned that the first clock in England was in Court Place Yard in Westminister in 1268. And then he started with the further development in 1639 by Galileo, who discovered the isochronal properties of oscillating bodies suspended by equal strings and hope that would apply in 1658 by Huygens to the suspended pendulum and things like that. And then he recalled the further developments of Hooke, Clemens, Grayham and Harrison.

Let us just continue then, Mr. Lockyer by 8 of diagram explained this successive improvement and then proceeded to exhibit in action a splended modern astronomical clock, loaned to him by Colonel Strange stating that the principles now demanded in such clocks are that the weight shall be small, and the pendulum heavy, and that there shall be as solid a connection between the two as possible. A word to the precautions necessary to be observed to preserve the pendulum from the action of temperature as much as possible in order to take advantage of the compensated pendulum. Then he went on to say, Mr. Lockyer then referred to Sir Charlie Whitstone's patent in 1840 to apply the electromagnetic force to record a very minute section of time and thought that

a tenth of a second or less they could do it that way. Then Mr. Lockyer concluded by demonstrating the great importance of photographs in that the determination of the longitude of distance places, such as Washington.

This was 111 years ago. I just wonder if anyone 111 years from today will read our proceedings; What's their opinions of our world, one hundred and eleven years from now?

INFLUENCE OF MODULATION FREQUENCY IN RUBIDIUM CELL FREQUENCY STANDARDS

C. AUDOIN and J. VIENNET
Laboratoire de l'Horloge Atomique
Equipe de Recherche du CNRS,
associée à l'Université Paris-Sud
Bât. 221 - Université Paris-Sud
91405 Orsay - France

and

N. CYR and J. VANIER
Laboratoire de Recherches sur les
Oscillateurs et les Systèmes
Département de Génie Electrique
Université Laval
Québec G1K7P4 - Canada

ABSTRACT

The error signal which is used to control the frequency of the quartz crystal oscillator of a passive rubidium cell frequency standard is considered. The value of the slope of this signal, for an interrogation frequency close to the atomic transition frequency is calculated and measured for various phase (or frequency) modulation waveforms, and for several values of the modulation frequency. A theoretical analysis is made using a model which applies to a system in which the optical pumping rate, the relaxation rates and the r.f. field are homogeneous*. Results are given for sine-wave phase modulation, square-wave frequency modulation and square-wave phase modulation. The influence of the modulation frequency on the slope of the error signal is specified. It is shown that the modulation frequency can be chosen as large as twice the non-saturated

*) *A typical experimental situation satisfying approximately these conditions is that of a small cell placed in the center of a* TE_{011} *cavity.*

full-width at half-maximum without a drastic loss of the sensitivity to an offset of the interrogation frequency from line center, provided that the power saturation factor and the amplitude of modulation are properly adjusted. The interest of square-wave phase modulation is pointed out for large modulation frequencies.
Experimental data has been obtained on a laboratory set-up in which a rubidium cell fills a TE_{111} microwave cavity.
Experimental results achieved with this configuration are in excellent agreement with the predictions of the given model.

1. INTRODUCTION

In passive frequency standards, such as the rubidium cell frequency standard, frequency control requires that the microwave interrogation signal is phase (or frequency) modulated. An error signal is obtained, which is proportional to the offset of the interrogation frequency from the line center, if this offset is small enough. The error signal drives the frequency control loop. The slope of this error signal has to be optimized in order to achieve the best frequency stability of the controlled quartz crystal oscillator. In practice, the modulation frequency should be large enough, i) to allow amplification of the modulated atomic cell response in a frequency range where shot noise dominates flicker noise and ii) to enable a reduction of the attack time of the frequency control loop, in order to ensure a better attenuation of the effect of perturbations, such as acceleration, which might affect the frequency of the quartz crystal oscillator.

Although investigation of frequency modulation effects has been performed by several authors in the framework of magnetic resonance experiments, very few analysis of frequency modulation has been given, which are directly applicable to the field of atomic frequency standards [1-4]. Furthermore, previous results are of limited practical interest because r.f. power saturation effects were not taken into consideration.

In this paper we give :

i) analytical expressions for the slope of the error signal assuming, at first, that the modulation is slow. Optimum values of the saturation factor and of the modulation depth are specified for sine-wave phase modulation and square-wave frequency modulation. The achieved results are used as a basis for further comparison with results derived when the dynamical behaviour of the atomic medium has to be taken into consideration i.e. when the modulation frequency is not small compared to the atomic line-width.

ii) analytical expressions for the slope of the error signal, for arbitrary values of the modulation depth and of the modulation frequency, but for weak saturation. We show that the results derived by Andres et al [1] and which were the only available for a long time are not exact.

iii) computed values of the slope of the error signal, for a large range of values of the saturation factor, the modulation depth and the modulation frequency. Sine-wave phase modulation, square-wave frequency modulation and square-wave phase modulation are considered. The influence of the value of the modulation frequency on the slope of the error signal is specified. The values of the saturation factor and of the modulation depth which maximizes the slope of the error signal are given.

iv) experimental values of the slope of the error signal for a rubidium cell filling a TE_{111} microwave cavity. Results are obtained for the three considered modulation waveforms. They confirm that the reduction of the error signal is small at modulation frequencies up to twice the non-saturated atomic line width.

2. THE MODEL USED FOR THE THEORETICAL ANALYSIS

In order to point out the results of major interest, we will consider a model in which the following simplifying assumptions are made.

i) the properties of the rubidium cell are homogeneous. This means that any effect related to the progressive absorption of light inside the atomic cell is neglected and that the light intensity is a constant across the light beam cross-section. In particular, the longitudinal and transverse relaxation times T_1 and T_2, respectively, will be assumed constant over the cell volume. Motional averaging in a coated cell without buffer gas would yield homogeneous values of T_1 and T_2.

ii) the microwave field is uniform over the rubidium cell volume. This condition is approximatively verified close to the center of a microwave cavity in which the TE_{011} mode is excited. On the contrary, the amplitude of the microwave field varies largely over the volume of a rubidium cell filling the entire volume of a TE_{111} cavity, an arrangement which is used widely in practice, in order to reduce the size of the frequency standard. However, we show in Section 7, that the experimental results are in very satisfactory agreement with the theoretical predictions and that, consequently, the model chosen is adequate.

iii) rubidium atoms behave as a two-level quantum system in which optical pumping has created the necessary population difference.

The given results are valid for passive frequency standards in which the atomic resonance is probed via a measure of the population difference between the two involved atomic levels. This measure consists either in the monitoring of the absorption of the pumping light, as in the passive rubidium cell frequency standard, or of the fluorescence of the optically pumped medium, as in the mass 199 mercury ion device.

Throughout this paper, we will assume that the following condition is fulfilled :

$$\omega_i - \omega_o << W \qquad (1)$$

where ω_i is the interrogation angular frequency*, ω_o is the atomic transition angular frequency and W is the full-width at half-maximum of the atomic resonance line (expressed in angular frequency unit).

The modulation depth will be characterized by a dimensionless parameter, u_2, defined as :

$$u_2 = T_2 \, \omega_m \tag{2}$$

where ω_m is the amplitude of the periodic angular frequency deviation.
Similarly, we will introduce the normalized modulation frequency v_2 defined as :

$$v_2 = T_2 \, \omega_M \tag{3}$$

where ω_M is the modulation angular frequency.
We will assume that synchronous detection consists in the multiplication of the fundamental component of the periodically modulated cell response by a demodulation function g'(t) such as :

$$g'(t) = \begin{cases} +1 \text{ for } 0 < t < T_M/2 \\ -1 \text{ for } T_M/2 < t < T_M \end{cases} \tag{4}$$

3. THE STATIC LINE SHAPE

It may be shown that the intensity I of the light transmitted by the rubidium cell is given by :

$$I = I_b + I_o \left[1 - \frac{S}{1+S+T_2^2 (\omega-\omega_o)^2}\right] \tag{5}$$

where I_b is a background component, I_o depends on the atomic density in the cell and on the properties of the light flux emitted by the rubidium lamp. The quantity S is the saturation factor defined as :

$$S = T_1 T_2 b^2 \tag{6}$$

where T_1 and T_2 are the longitudinal and transverse relaxation times, respectively and b is a measure of the microwave field applied to rubidium atoms.

Equation (5) describes the resonance line as a lorentzian function of the difference between the angular frequency ω of the microwave field and the angular transition frequency ω_o. The full-width-half-maximum of the line, W, is given by :

---

*) *The interrogation frequency is the mean value of the modulated instantaneous frequency. Therefore, equation (1) does not mean that we restrict ourself to small time dependent frequency deviations. On the contrary, we will consider frequency excursions which are of the order of magnitude of the atomic line-width.*

$$W = \frac{2}{T_2} \sqrt{1+S} \tag{7}$$

and the height of the resonance line is I_ℓ such as :

$$I_\ell = - I_o \frac{S}{1+S} \tag{8}$$

where the minus sign indicates that the resonance appears as a dip in the transmission profile of the resonance cell. For very large values of S, we have $I_\ell = - I_o$.

4. THE NORMALIZED SLOPE OF THE ERROR SIGNAL

The error signal, which is useful for frequency control of the quartz crystal oscillator is proportional to the low-pass component of the synchronous detector output. Under the condition given by equation (1), it is proportional to the angular frequency offset of the interrogation frequency from the line center. We then define the following normalized slopes of the error signal for $(\omega_i - \omega_o) << W$:

i) $$p = \frac{\overline{I_p(t) g'(t)}}{I_o T_2 (\omega_i - \omega_o)} \tag{9}$$

where $I_p(t)$ is the component of the fundamental of the cell response which is in phase with the modulation waveform. The bar means time average.

ii) $$q = \frac{\overline{I_q(t) g'(t)}}{I_o T_2 (\omega_i - \omega_o)} \tag{10}$$

where $I_q(t)$ is the component of the fundamental of the cell response which is in quadrature with the modulation waveform.

iii) $$a = (p^2 + q^2)^{1/2} \tag{11}$$

This is the slope of the error signal when the phase of the fundamental of the cell response and of the demodulation signal are matched.

5. SLOW FREQUENCY MODULATION

In the condition of slow frequency modulation, the period $T_M = 2\pi/\omega_M$ of the frequency modulation is large compared to the atomic longitudinal and transverse relaxation times. We then have :

$$v_2 \simeq 0 \tag{12}$$

In this quasi static approximation, the atomic medium is assumed to reach a steady state for every value of the angular frequency ω of the applied microwave field. Equation (5) is then valid, with ω depending on time.

5.1. Square-wave frequency modulation

The instantaneous angular frequency $\omega(t)$ is given by :

$$\omega(t) = \omega_i + \omega_m g(t) \tag{13}$$

where g(t) is the modulation function which describes the frequency modulation waveform. For square-wave frequency modulation, it is given by :

$$g(t) = \begin{cases} +1 & 0 < t < T_M/2 \\ -1 & T_M/2 < t < T_M \end{cases} \tag{14}$$

It can easily be seen that under condition (1), the fundamental component of the modulated light intensity, which is transmitted by the rubidium cell is in phase with the frequency modulation waveform.
We have :

$$I_p(t) = \frac{8}{\pi} I_o \frac{S u_2 T_2(\omega_i - \omega_o)}{(1+S+u_2^2)^2} \sin \omega_M t \tag{15}$$

The fundamental component of the demodulation waveform g'(t) being $(4/\pi)\sin \omega_M t$, the normalized slope a of the error signal is given by :

$$a = \frac{16}{\pi^2} \frac{S u_2}{(1+S+u_2^2)^2} \tag{16}$$

It can easily be shown that the maximum value of a = 0.203 occurs for S = 2 and $u_2 = 1$. These values define the optimum operating conditions for applied microwave power and modulation depth. Figure 1a shows the variation of a versus the quantity u_2 for different values of S.

5.2. Sine-wave frequency modulation

The frequency modulation waveform function g(t) of equation (13) is now :

$$g(t) = \sin \omega_M t \tag{17}$$

The fundamental component of the transmitted light intensity can be either derived directly thanks to standard techniques of calculation of the coefficients of the Fourier series expansion of the response, or using general results obtained by Arndt [5] who has analyzed the quasi-static sine-wave frequency modulation of a lorentzian line.

The fundamental of the cell response is in phase with the frequency modulation waveform, and we have :

$$a = \frac{4}{\pi} \frac{S u_2}{(1+S)^{1/2}(1+S+u_2^2)^{3/2}} \tag{18}$$

The maximum value of a = 0.189 is achieved for S = 2, as in the previous case, but for $u_2 = 1.22$. Figure 1b shows the variation of a versus the quantity u_2 for different values of S.

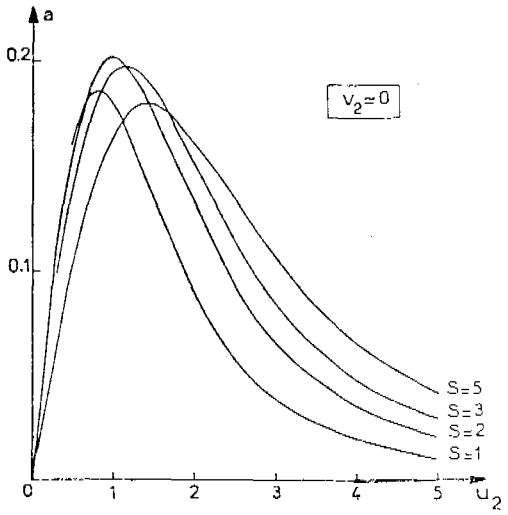

Fig. 1a

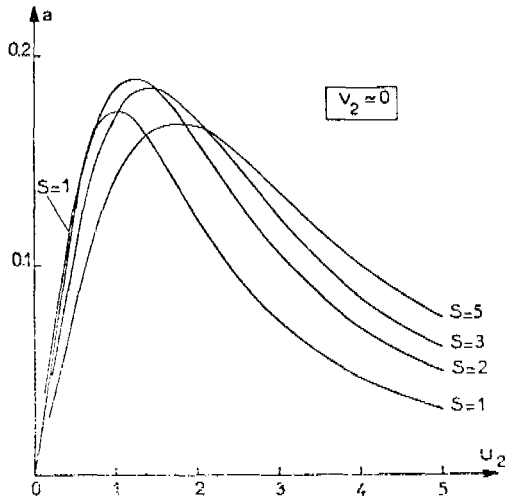

Fig. 1b

Fig. 1. Quasi static approximation. Variation of the normalized slope a of the error signal versus the normalized modulation depth $u_2 = T_2\omega_m$ for different values of the saturation factor S, in the quasi-static approximation.

a) square-wave frequency modulation with narrow band filtering of the response, at the modulation frequency.

b) sine-wave frequency modulation with narrow band filtering of the response, at the modulation frequency.

6. INFLUENCE OF THE MODULATION FREQUENCY ON THE SLOPE OF THE ERROR SIGNAL

6.1. Bloch equation of the modulation problem

In general, the behaviour of any two level quantum system which follows assumptions i) to iii) of Section 2 can be described by Bloch equations [6]. For a $\Delta F = 1$, $\Delta m_F = 0$ transition, as used in an atomic frequency standard, those equations are best expressed in terms of the so-called coherence of the atomic medium, a(t), and of the population difference between the two atomic levels, $a_3(t)$. The quantity a(t) is a complex one, and we set $a(t) = a_1(t) + ia_2(t)$.

It can be shown that, in the presence of modulation, the Bloch equations of the considered problem are the following :

$$T_2\dot{a}_1 + a_1 + T_2(\omega_i-\omega_o)a_2 = T_2\ b\ a_3 \sin\varphi$$

$$T_2\dot{a}_2 + a_2 - T_2(\omega_i-\omega_o)a_1 = T_2\ b\ a_3 \cos\varphi \qquad (19)$$

$$T_1\dot{a}_3 + a_1 = \lambda T_1 - T_1 b(a_1 \sin\varphi + a_2 \cos\varphi)$$

where the dot means time derivative. The quantity λ is the creation rate of the population difference which in the present case is obtained by optical pumping. The time dependent quantity φ is the instantaneous phase of the microwave interrogation signal, and the instantaneous angular frequency is :

$$\omega(t) = \omega_i + \dot{\varphi} \qquad (20)$$

The quantity of interest to us is the population difference $a_3(t)$ merely because the transmitted light intensity changes are proportional to $a_3(t)$. We will consider the fundamental component of $a_3(t)$ in the presence of specified phase modulation waveforms. From now on, the in phase and in quadrature components of the fundamental of the cell response will be referred to the *phase* modulation waveform rather than to the *frequency* modulation waveform.
A look at equations (19) shows the following :

i) they are coupled to a degree which depends on the microwave field amplitude b, and thus of the saturation factor S

ii) the driving terms in their right hand sides are periodic functions of time which need to be represented by Fourier series with in general an infinite number of terms. Equations (19) then generate, in general, an infinite set of coupled equations.

Consequently, it is not tractable to derive analytical solutions for the quantity a_3, unless simplifying assumptions are made. One of them is the weak saturation assumption which will be considered in Section 6.2. Equations (19) have also been analytically solved for arbitrary saturation, but under the assumption of fast modulation, for which the spectrum of the cell response can be limited to frequencies $-\omega_M$, 0 and $+\omega_M$. The related results will be published elsewhere.

For operating conditions prevailing in rubidium cell frequency standards, equations (19) must be solved by numerical techniques. The results are given in Section 6.3.

6.2. Analytical solution for weak saturation

As it will be shown later, operating conditions are optimized for saturation factors larger than unity. However, we wish to consider weak saturation (i.e. $S \ll 1$) at first with the purpose of pointing out that one should not rely on previously published results [1] established under this assumption.

In quantum electronics, it is usual practice to expand the quantities such as a_1, a_2 and a_3 in increasing powers of the field amplitude, and to derive solutions for components of a given degree. However, the equations obtained are more and more intricated as the degree of the considered component increases.

We will limit the expansion to degree two of field amplitude, i.e. to degree one of saturation factor. The validity of the results is then limited to small values of S, i.e. $S \ll 1$.

This perturbation expansion has been considered for sine-wave phase modulation, square-wave frequency modulation and square-wave phase modulation [4]. We will focus here on sine-wave phase modulation.

We define the slopes $p^{(2)}$ and $q^{(2)}$ of the error signal when the fundamental of the cell response is observed in phase or in quadrature with respect to the phase modulation waveform. The superscript means that results are valid to order two of field amplitude only. It comes :

$$\frac{1}{S}\, p^{(2)} = \frac{v_1}{1+v_1^2}\,\alpha'_1 + \frac{1}{1+v_1^2}\,\alpha'_2 \tag{21a}$$

$$\frac{1}{S}\, q^{(2)} = \frac{1}{1+v_1^2}\,\alpha'_1 - \frac{v_1}{1+v_1^2}\,\alpha'_2 \tag{21b}$$

where we have $v_1 = T_1\omega_M$ and where the quantities α'_1 and α'_2 are given by the following equations :

$$\alpha'_1 = \frac{8}{\pi} \sum_{\ell=1}^{\infty} \frac{\ell v_2}{(1+\ell^2 v_2^2)^2} \left[J_{\ell+1}(m) + J_{\ell-1}(m)\right] J_\ell(m) \tag{22a}$$

$$\alpha'_2 = \frac{4}{\pi} \left\{ J_o(m) J_1(m) + \sum_{\ell=1}^{\infty} \frac{1-\ell^2 v_2^2}{(1+\ell^2 v_2^2)^2} \left[J_{\ell+1}(m) - J_{\ell-1}(m)\right] J_\ell(m) \right. \tag{22b}$$

J_ℓ is Bessel function of order ℓ. The quantity m is the phase modulation index such as $m = \omega_m/\omega_M$. ℓ is an integer.

In practice relaxation times T_1 and T_2 have values which are very close together, in the considered atomic medium. In order to derive general information on the slope of the error signal, we set :

$$T_1 = T_2 = T \tag{23}$$

in equations 21 and 22.
We then have : $v_1 = v_2 = v = T\omega_M$ and $u_2 = u = T\omega_m$. The phase modulation index is $m = u/v$.

Figures 2a and b show the variations of $p^{(2)}$ and $q^{(2)}$, respectively, versus the normalized modulation frequency v for different values of the normalized modulation depth u. These sets of curves differ significantly from that given by Andres et al [1]. An examination of their derivation shows that the longitudinal relaxation was not properly accounted for. In figures 2a and b, the undulations are related to additional resonance features which occurs at frequencies $\omega_o \pm \ell\omega_M$, in the presence of periodic phase modulation.

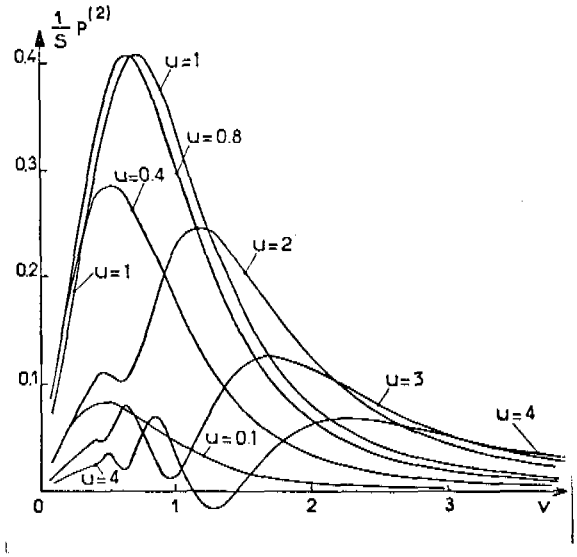

Fig. 2a

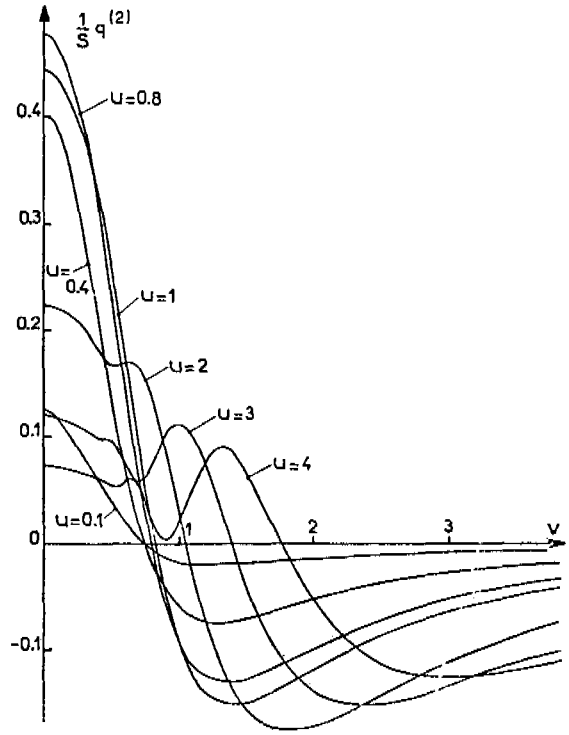

Fig. 2b

Fig. 2. Sine-wave phase modulation and weak saturation (S << 1). The curves show the variation of the slope of the error signal versus the normalized modulation angular frequency $v = T\omega_M$ and for different values of the normalized modulation depth $u = T\omega_m$.

a) the fundamental of the cell response is observed in phase with the phase modulation waveform.

b) the fundamental of the cell response is observed in quadrature with the phase modulation waveform.

6.3. Computed results for values of the modulation frequency of the modulation depth and of the saturation factor in ranges of practical interest

The set of equations (19) has been integrated numerically, assuming $T_1 = T_2 = T$ for sine-wave phase modulation, square-wave frequency modulation and square-wave phase modulation. The quantity $(\omega_i - \omega_o)$ has been fixed to a value which equals 1/10 of the half-width at half-maximum of the non-saturated resonance line (i.e. $T_2(\omega_i - \omega_o) = 0.1$). It has been checked that this offset is small enough that it allows a precise enough calculation of the slope of the error signal, and of the phase of the fundamental of the cell response, for $\omega_i = \omega_o$. Physically sound initial conditions have been chosen and the numerical integration has been performed until transient

effects vanish. The components of the fundamental of the population difference change which are in phase and in quadrature with the modulation waveform are extracted using standard techniques of Fourier coefficients computation. The values of the slopes p and q are then derived. Physically, they are obtained when the fundamental of the cell response is observed in phase or in quadrature with respect to the phase modulation waveform.

In the following we will give the values of the slope a , defined by equation (11), which is obtained when the reference signal applied to the synchronous detector is delayed in order to match its phase to that of the fundamental component of the cell response. The phase of this fundamental, relative to the phase modulation waveform is ϕ given by :

$$\tan \phi = \frac{q}{p} \tag{24}$$

Double precision computation techniques have been used to derive numerical results. Furthermore, it has been checked that the computed results agree with analytical ones, in the limits of weak saturation, or fast frequency modulation, for the three considered types of phase modulation.

6.3.1. Results for sine-wave phase modulation

Figures 3a to 3e show the computed variation of the slope a of the error signal and of the phase ϕ of the fundamental of the population difference change versus the normalized modulation depth $u = T\omega_m$ for different values of the saturation parameter $S = T_1 T_2 b^2$, which is proportional to the microwave power. Figures differ by the value of the normalized modulation frequency $v = T\omega_M$.

On figure 3a established for a relatively slow frequency modulation such as $v = 0.1$, the circles represent values calculated under the quasi-static approximation i.e. for $v = 0$, according to equation(18). For $v \simeq 0$, the fundamental of the population difference change is in quadrature with the phase modulation of the interrogation microwave field. One sees that the validity of the quasi-static approximation is extremely good for $v = 0.1$.

Figures 3a to 3e are for increasing values of the modulation frequency. The origin of the undulations is the same as in figures 2a and 2b.

Table 1 gives, for specified values of the normalized modulation frequency v, the values of the saturation factor S and of the normalized modulation depth u for which the slope a of the error signal is a maximum. It shows off the main result : the slope of the error signal does not depend strongly on the modulation frequency provided that the saturation factor and the modulation depth are properly increased as the modulation frequency takes larger values. For instance, for $v = 1.9$, i.e. for a modulation frequency almost equal to the non-saturated full-width- at half-maximum, the slope a may be made equal to its value for slow frequency modulation. It may also be noticed that the loss in the value of the slope remains small for $v \simeq 4$.

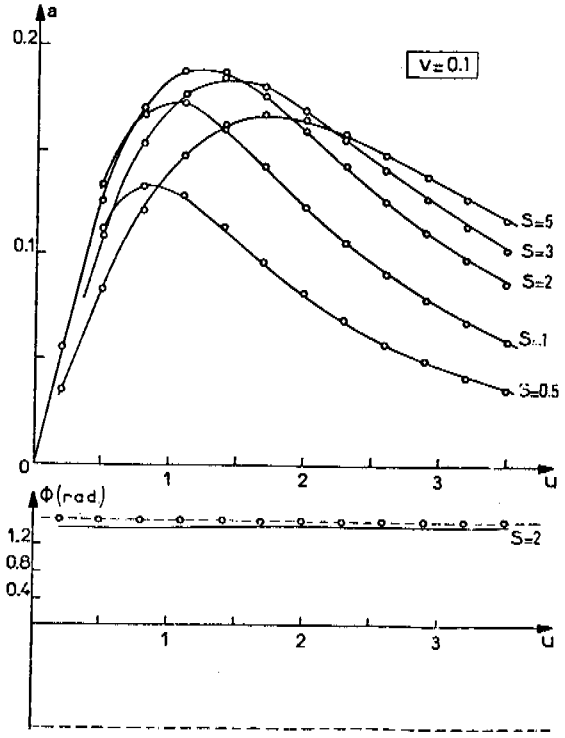

Fig. 3a

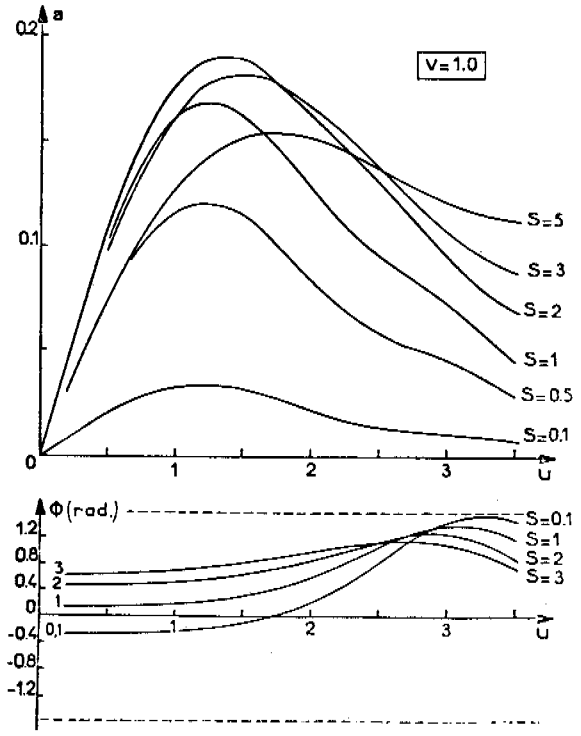

Fig. 3b

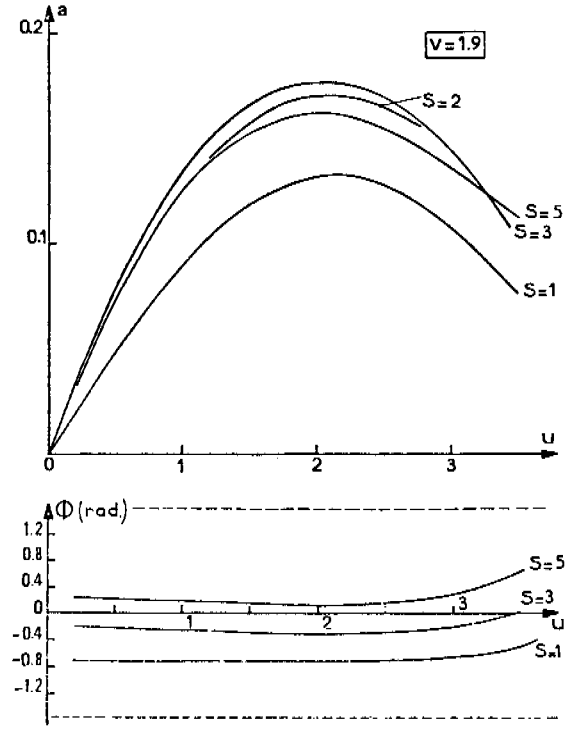

Fig. 3c

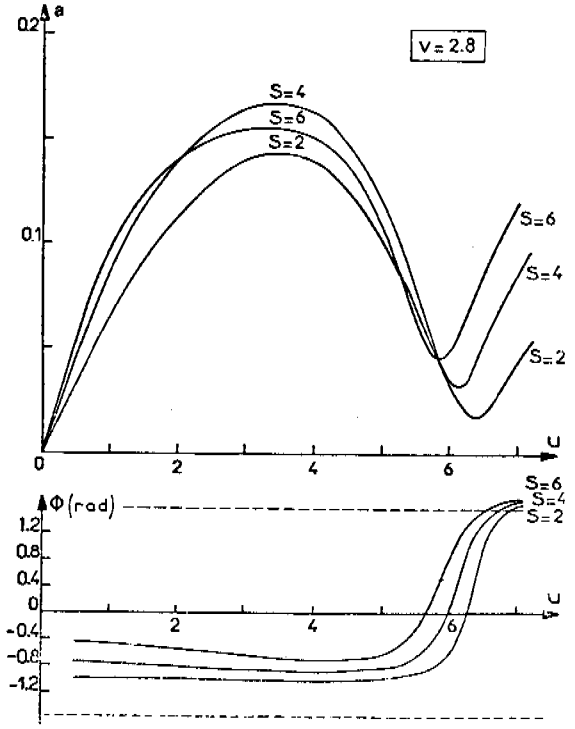

Fig. 3d

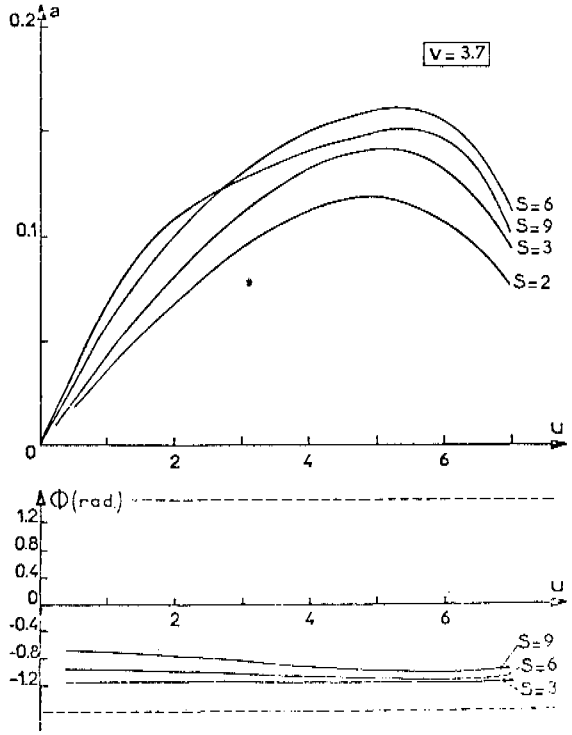

Fig. 3e

Fig. 3. Sine-wave phase modulation *computed results*. Variation of the slope of the error signal and of the phase ϕ, versus the normalized modulation depth u and for different values of the saturation factor S.

a) v = 0.1. Circles represent the values calculated under the quasi static approximation, according to equation (18).
b) v = 1.0
c) v = 1.9
d) v = 2.8
e) v = 3.7

v	S	u	a	ϕ
0	2.0	1.22	0.189	1.57
0.1	2 ($\pm$ 1)	1.1 ($\pm$ 0.3)	0.187	1.47
1.0	2 ($\pm$ 1)	1.4 ($\pm$ 0.3)	0.190	0.60
1.9	3 ($\pm$ 1)	2.0 ($\pm$ 0.3)	0.189	- 0.30
2.8	4 ($\pm$ 1	3.5 ($\pm$ 0.5)	0.166	- 0.87
3.7	6 ($\pm$ 1)	5.5 ($\pm$ 0.5)	0.160	- 1.10

Table 1. Sine-wave phase modulation *computed values*. For a given value of the normalized modulation frequency v, the slope a of the error signal shows a maximum for the specified values of the saturation factor S and of the normalized modulation depth u.
For v = 0, results are derived from the quasi-static approximation. The quoted uncertainties on S and u are equal to the step of change of these parameters in the computations made. The phase ϕ is expressed in radian.

6.3.2. Results for square-wave frequency modulation

Figure 4 shows an example of the computed variation of the slope a of the error signal and of the phase ϕ of the fundamental of the population difference change versus the normalized modulation depth u, for different values of the saturation parameter S.

Table 2 gives, for specified values of the normalized modulation frequency v, the values of the saturation factor S and of the normalized modulation depth u for which the slope a of the error signal shows a maximum.

For v = 0.1, the computed results are closely identical to the results obtained under the quasi-static approximation, and given by equation (16). The same sort of remarks and conclusions which have been made for sine-wave phase modulation apply for square-wave frequency modulation.

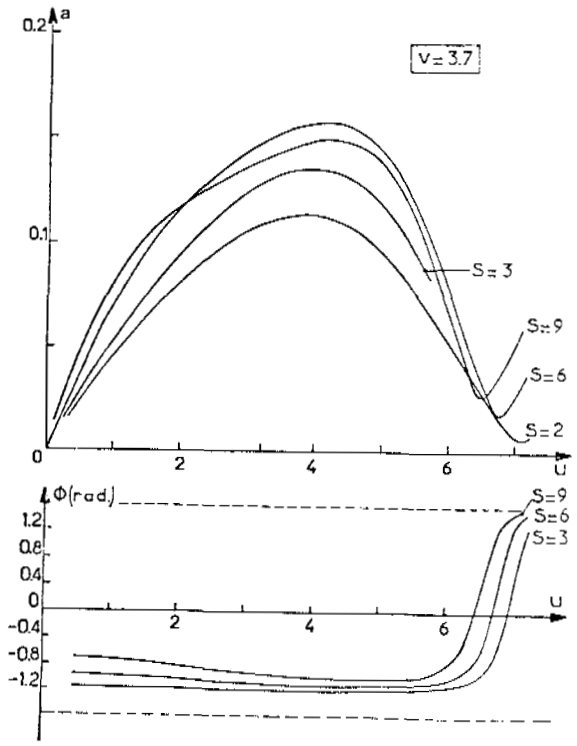

Fig. 4. Square-wave frequency modulation *computed results*. Variations of the slope a of the error signal and of the phase ϕ, for v = 3.7, versus the normalized modulation depth u and for different values of the saturation factor S.

v	S	u	a	ϕ
0	2.0	1.0	0.203	1.57
0.1	2 ($\pm$ 1)	1.1 ($\pm$ 0.3)	0.201	1.47
1.0	2 ($\pm$ 1)	1.1 ($\pm$ 0.3)	0.197	0.59
1.9	3 ($\pm$ 1)	1.7 ($\pm$ 0.3)	0.178	- 0.30
2.8	4 ($\pm$ 1)	2.5 ($\pm$ 0.5)	0.163	- 0.85
3.7	6 ($\pm$ 1)	4.0 ($\pm$ 0.5)	0.157	- 1.09

Table 2. Square-wave frequency modulation *computed values*. For a given value of the normalized modulation frequency v, the slope a of the error signal shows a maximum for the specified values of the saturation factor S and of the normalized modulation depth u. For v = 0, results are derived from the quasi-static approximation. The quoted uncertainties on S and u are equal to the step of change of these parameters in the computations made. The phase ϕ is expressed in radian.

6.3.3. Results for square-wave phase modulation

For square-wave phase modulation, the atomic medium response is entirely founded on transient effects which occur after phase jumps. In that case, the quasi-static approximation is then meaningless, because the first harmonic content of the cell response vanishes for $v \simeq 0$. Intuitively, one might think that the cell response is significant when the modulation frequency is of the order of the atomic line-width. This is verified, in order of magnitude, by quantitative results.

Figures 5a to 5d show the computed variations of the slope a of the error signal and of the phase ϕ of the fundamental of the population difference change versus the amplitude of the phase deviation φ_m, for different values of the saturation parameter S (it should be noticed that the phase steps amount to $2\varphi_m$). Figures differ by the value of the normalized modulation frequency v.

Table 3 summarizes the important results. It gives for the specified values of the normalized modulation frequency v, the values of the saturation factor and of the amplitude of the phase change φ_m for which the slope a of the error signal shows a maximum. The optimum value of φ_m is close to $\pi/4$. This slope decreases only very slightly from $v \simeq 1.9$ to 3.7, in the explored range, when the saturation factor S and the phase change φ_m are adjusted to their increasing optimum values.

v	S	φ_m	a	ϕ
1.0	2 ($\pm$ 1)	0.8 ($\pm$ 0.1)	0.148	0.44
1.9	3 ($\pm$ 1)	0.8 ($\pm$ 0.1)	0.171	- 0.42
2.8	4 ($\pm$ 1)	1.0 ($\pm$ 0.1)	0.170	- 0.97
3.7	7 ($\pm$ 1)	1.1 ($\pm$ 0.1)	0.169	- 1.15

Table 3. Square-wave phase modulation *computed values*. For a given value of the normalized modulation frequency v, the slope a of the error signal shows a maximum for the specified values of the saturation factor S and of the amplitude of phase deviation φ_m. The quoted uncertainties on the values of these parameters are equal to their step of change in the computations made. The phases φ_m and ϕ are expressed in radian.

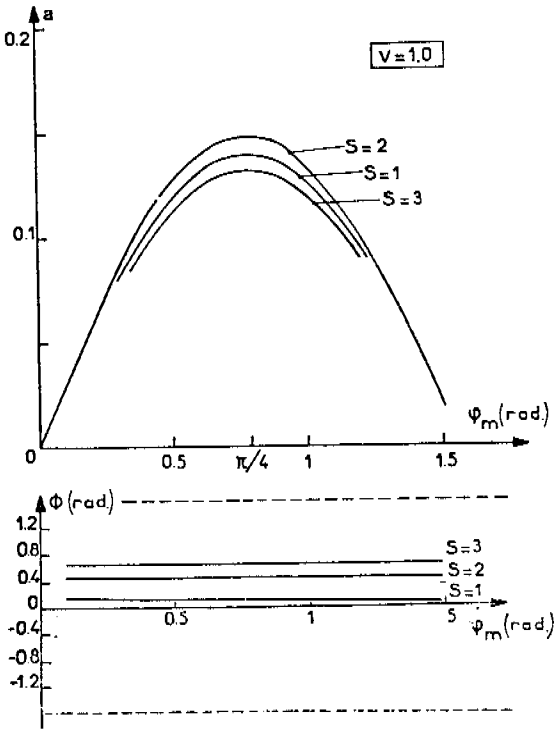

Fig. 5a

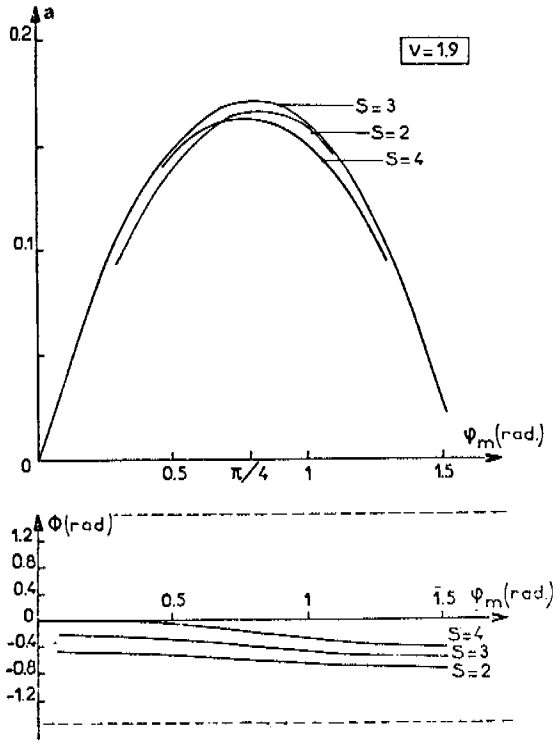

Fig. 5b

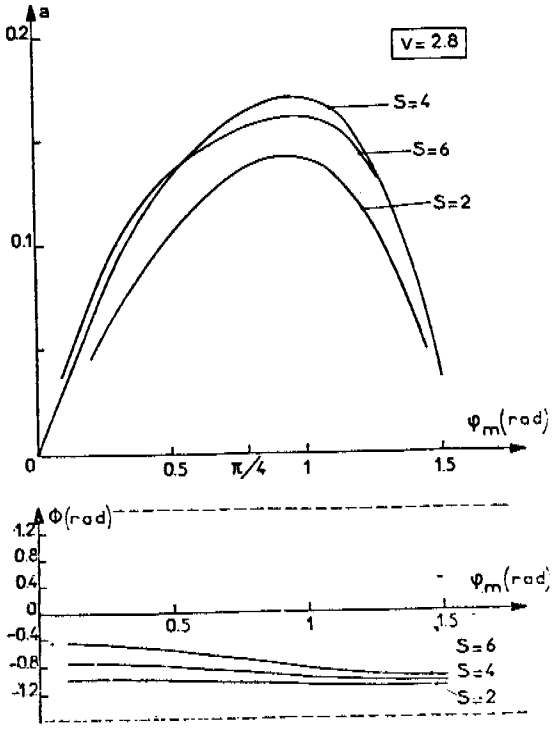

Fig. 5c

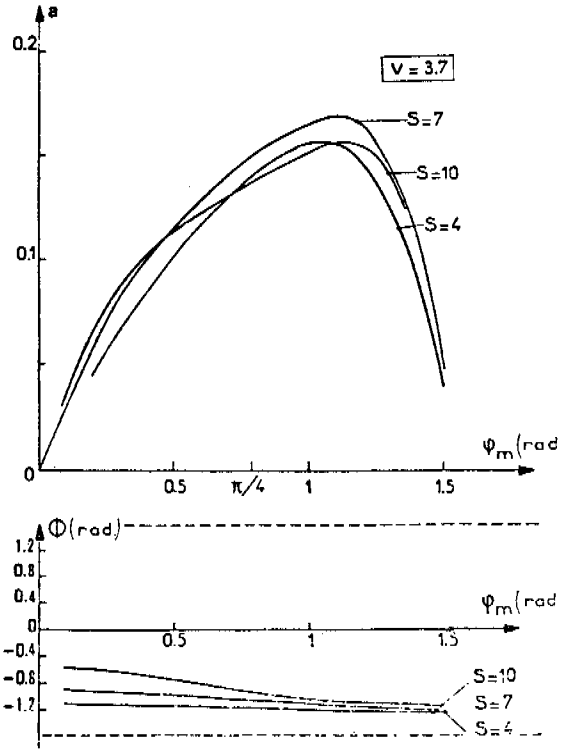

Fig. 5d

Fig. 5. Square-wave phase modulation *computed results*. Variation of the slope a of the error signal and of the phase ϕ, versus the amplitude of the phase change φ_m and for different values of the saturation factor S.
a) v = 1.0
b) v = 1.9
c) v = 2.8
d) v = 3.7

7. EXPERIMENTAL RESULTS

Experimental results have been obtained with a set-up having a widely used configuration. An isotopic filter, with 80 Torrs of argon is used. The Rb^{87} cell containing 20 Torrs of nitrogen is operated at 60° C. It fills almost entirely a cylindrical microwave cavity operated in the TE_{111} mode. In this experimental arrangement, optical pumping and relaxation are not homogeneous in the cell. In addition the microwave magnetic field amplitude shows large variations over the cell volume. The experimental results can then be used to check the ability of our model to predict the influence of the modulation frequency on a practical device.

An average saturation factor S' is defined from the dip of the transmitted light at microwave resonance. We have, from equation (8) :

$$S' = - I_\ell/(I_0 + I_\ell) \tag{25}$$

The value of the transverse relaxation time T_2 is measured by extrapolating the atomic line-width to zero microwave power. It is found that the full-width at half maximum W varies as follows :

$$W^2 = W_0^{\,2}(1 + \alpha S') \tag{26}$$

where $W_0 = 2/T_2$ is the non-saturated linewidth. Experimentally, one has $\alpha = 5.2^0$ and

$$T_2 = 1.77 \pm 0.18 \text{ ms}$$

It can be shown that the value of α depends on the microwave field configuration, the light intensity, the length of the cell, the temperature and also on the area of the photo cell exposed to the transmitted light.

The value of the longitudinal relaxation time is measured by observing the exponential variation of the transmitted light intensity after the microwave power has been switched off. We have

$$T_1 = 1.82 \pm 0.04 \text{ ms}$$

Thus it turns out that the condition $T_1 = T_2$ which has been assumed in Section 6.3. is fulfilled quite satisfactorily.

The slope of the error signal is measured as follows. A quartz crystal oscillator is frequency locked to the rubidium cell, but with a voltage added to the synchronous detector output. The frequency of the quartz crystal oscillator is measured for two opposite values of the voltage, and the normalized slope of the error signal is obtained. It has been checked that the offset of the interrogation frequency from the resonance frequency remained smaller than 1/10 of the full-width at half-maximum. The phase of the fundamental component of the light intensity changes shows an extremum for $\omega_i = \omega_o$, so that its measurement was precise enough with the stated experimental procedure.

Sine-wave phase modulation, square-wave frequency modulation and square-wave phase modulation have been applied to the microwave signal.

Figures 6a to 6d show the results for sine-wave phase modulation. The value of the measured slope is smaller than the value calculated from the model, and the optimum occurs for smaller values of the saturation factor (for v = 0.1 the optimum value of S' is 1.3). However, for a given value of v, the shape of the computed and of the measured variations is quite similar. Table 4 summarizes the experimental results. It shows that the optimum value of a does not depend drastically on the value of the modulation frequency.

v	S'	u	a x 10^2	ϕ
0.11	1(± 0.5)	1.3 ± 0.1	9.3	1.48
1	1(± 0.5)	1.5 ± 0.15	8.6.	0.58
2.9	1.5(± 0.5)	3.5.± 0.25	5.6	- 0.51
3.7	2(± 0.5)	4.2 ± 0.25	5.1	- 0.72

Table 4. Sine-wave modulation. *Experimental values*. For a given value of the normalized modulation frequency v, the slope a of the error signal shows a maximum for the specified values of the saturation factor S' and of the normalized modulation depth u. The quoted uncertainties on S' and u are equal to the step of change of these parameters in the measurements made. The phase ϕ is expressed in radian.

Figure 7 shows an example of measured results for square-wave frequency modulation with v = 3.7 and Table 5 gives the main results, with the same general conclusions as for sine-wave phase modulation.

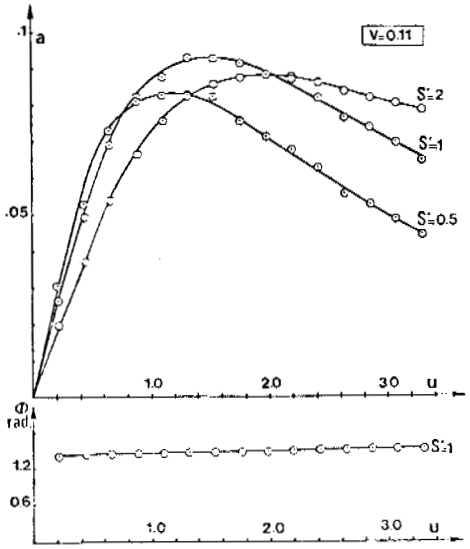

Fig. 6a

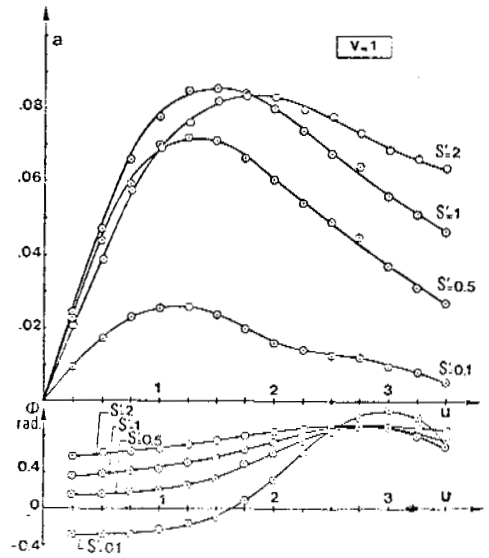

Fig. 6b

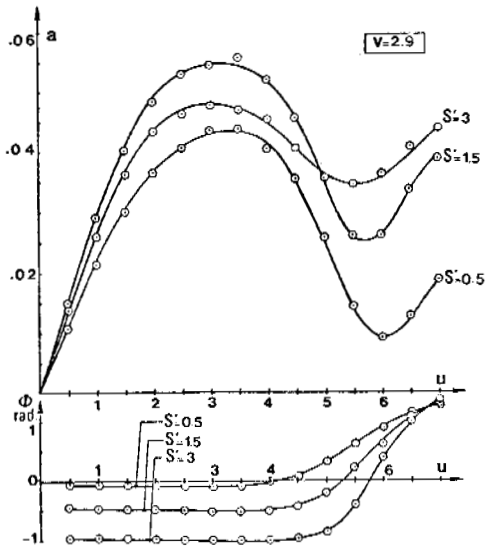

Fig. 6c

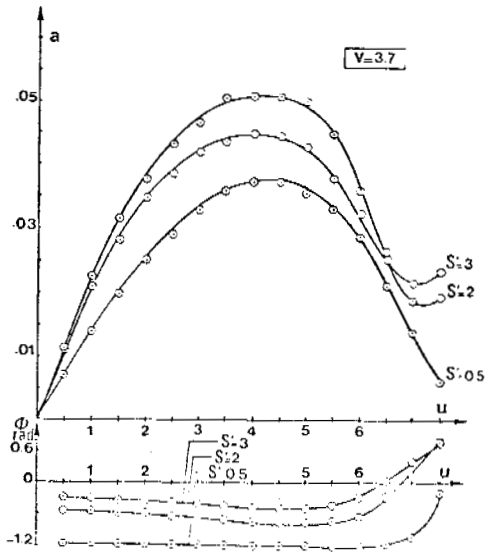

Fig. 6d

Fig. 6. Sine-wave phase modulation. *Experimental results.* Variation of the slope a of the error signal and of the phase ϕ, versus the normalized modulation depth u and for different values of the saturation factor S'. Circles represent the experimental points.
a) v = 0.11 b) v = 1.0
c) v = 2.9 d) v = 3.7

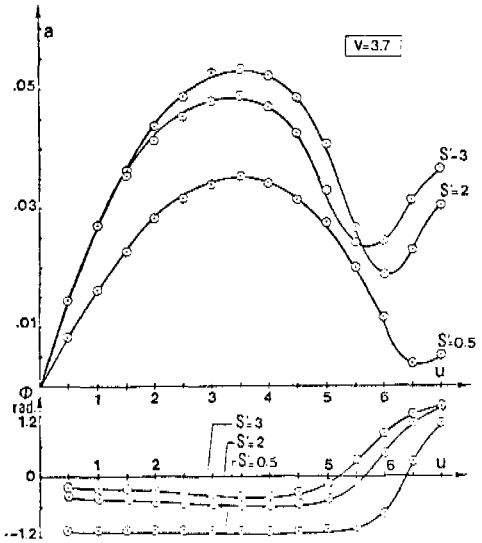

Fig. 7. Square-wave frequency modulation. *Experimental results*. Variation of the slope a of the error signal and of the phase ϕ, for v = 3.7, versus the normalized modulation depth u and for different values of the saturation factor S'. Circles represent the experimental points.

v	S'	u	a x 10^2	ϕ
0.2	1 ($\pm$0.5)	1.1 $\pm$ 0.15	10.0	1.52
1	1 ($\pm$0.5)	1.25 $\pm$ 0.15	8.6	0.79
2.9	1.5($\pm$0.5)	2.5 $\pm$ 0.25	5.9	- 0.38
3.7	2 ($\pm$0.5)	3.5 $\pm$ 0.25	5.3	- 0.60

Table 5. Square-wave frequency modulation. *Experimental values*. For a given value of the normalized modulation frequency v, the slope a of the error signal shows a maximum for the specified values of the saturation factor S' and of the normalized modulation depth u. The quoted uncertainties on S' and u are equal to the step of change of these parameters in the measurements made. The phase ϕ is expressed in radian.

Figures 8a to 8c show the variation of the normalized slope a in the case of square-wave phase modulation as a function of the amplitude of the phase deviation φ_m for different values of the saturation factor S' and of the normalized modulation frequency v. Again, the shapes agree quite satisfactorily, but with smaller values of a and S'. Table 6 shows that the optimum values of φ_m agree closely with the computed ones.

Comparison of Tables 4 to 6 shows that square-wave phase modulation yields an optimum value of the slope a which is even larger than with the two other types of modulation for v ≃ 4.

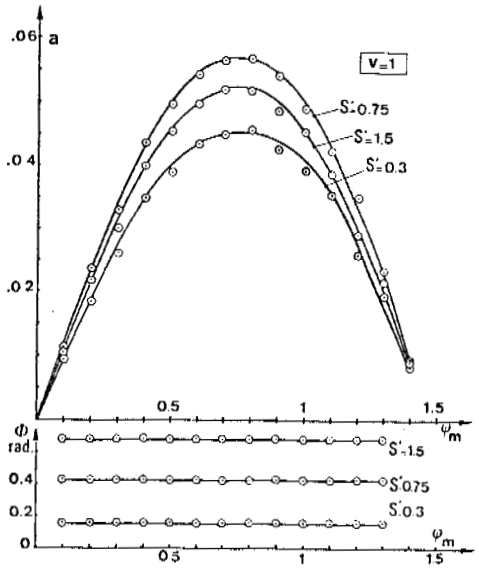

Fig. 8a

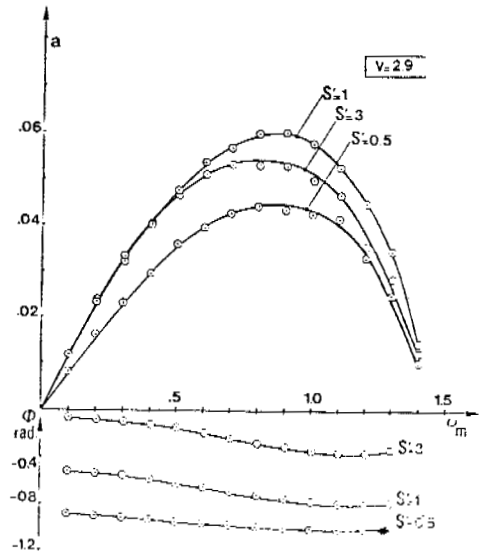

Fig. 8b

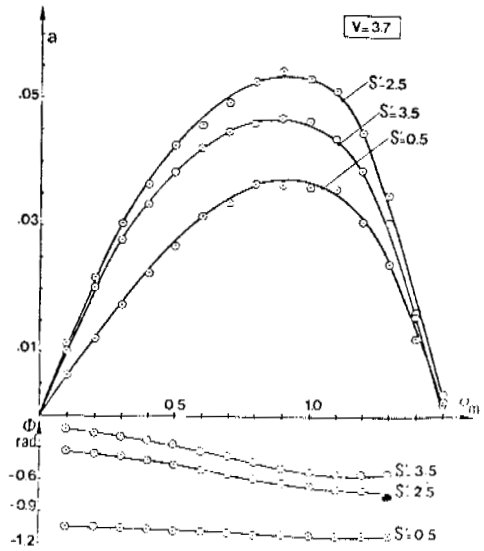

Fig. 8c

Fig. 8. Square-wave phase modulation. *Experimental results*. Variation of the slope a of the error signal and of the phase ϕ, versus the normalized modulation depth u and for different values of the saturation factor S'. Circles represent the experimental points.
a) v = 1.0
b) v = 2.9
c) v = 3.7

v	S'	φ_m	a x 10^2	ϕ
1	0.75 ($\pm$0.5)	0.8 $\pm$ 0.5	5.7	0.44
2.9	1 ($\pm$0.5)	0.9 $\pm$ 0.5	6.0	- 0.75
3.7	2.5 ($\pm$0.5)	0.95 $\pm$ 0.5	5.5	- 0.63

TABLE 6. Square-wave phase modulation. *Experimental values*. For a given value of the normalized modulation frequency v, the slope a of the error signal shows a maximum for the specified values of the saturation factor S' and of the amplitude of phase deviation φ_m. The quoted uncertainty on the values of these parameters are equal to their step of change in the computations made. The phases φ_m and ϕ are expressed in radian.

8. CONCLUSIONS

Our theoretical analysis has been made with the assumption that optical pumping, relaxation and the r.f. field are homogeneous over the rubidium cell. Our experimental data has been obtained with a rubidium cell in a TE_{111} cavity and those conditions are not satisfied. However, these results agree satisfactorily with the theoretical predictions. Consequently, we may conclude the following :

i) for sine-wave phase modulation and square-wave frequency modulation, the results of the quasi-static approximation can be used up to $v \simeq 1$, as far as the slope a of the error signal is concerned. It yields a satisfactory estimate of the values of the saturation factor and of the normalized modulation depth for which this slope is maximum.

ii) for sine-wave phase modulation and for square-wave frequency modulation, the slope a of the error signal decreases only slightly if the modulation frequency is increased up to a value such as $v \simeq 4$, provided that the saturation factor and the modulation depth are adjusted to increasing optimum values specified in Tables 1 and 2. One sees that when the modulation frequency increases, the line must be power broadened in order that the linewidth tends to follow the value of the modulation frequency. Similarily, the frequency excursion around the interrogation frequency has to be increased.

iii) for square-wave phase modulation, the optimum modulation frequency is such as $v \simeq 2$ and the slope a falls off very slightly for $v \gtrsim 2$ when the values of the saturation factor and of the amplitude of the periodic phase change are adjusted to the values given in Tables 3 or 6.

iv) for large modulation frequency such as $v \simeq 4$, the slope a becomes a little larger for square-wave phase modulation than for the two other sorts of modulation which have been considered. Square-wave phase modulation might then be the best modulation method in applications where fast

frequency modulation is required. In addition, it has other known specific advantages such as ease of implementation and excellent immunity to non-linear distortion of the phase modulator.

REFERENCES

[1] J.M. Andres, D.J. Farmer and G.T. Inouye, IRE Trans. on Military Electronics 3 (1959) p. 178-183

[2] R.P. Kenschaft, Ph. D. (1970)University of Pennsylvania

[3] G. Missout and J. Vanier, Canadian Journal of Physics 53 (1975) p. 1030-1043

[4] P. Thomann and G. Busca, Journal de Physique. Supplément au n° 12. Colloque C8 (1981) p. C8-189 - C8-197

[5] R. Arndt, Journal of Applied Physics 36 (1965) p. 2522-2524

[6] A. Abragam, Principles of Nuclear Magnetism, Clarendon Press (1962)

QUESTIONS AND ANSWERS

(Signals inadequate for transcription for Paper #4.)